e-ISSN: 0975-1556, p-ISSN:2820-2643

Available online on www.ijpcr.com

International Journal of Pharmaceutical and Clinical Research 2023; 15(7); 1184-1194

Original Research Article

Ex-Vivo Permeation Study of an Antifungal Drug, Loaded in NLC, Designed and Optimized by Factorial Design

Gopa Roy Biswas, Soumik Patra, Pakhi Chakraborty, Pritam Dutta, Grihadeep Paul

Department of Pharmaceutics, Guru Nanak Institute of Pharmaceutical Science and Technology, 157/F Nilgunj Road, Panihati, Sodepur, Kolkata-700114

Received: 10-05-2023 / Revised: 10-06-2023 / Accepted: 10-07-2023
Corresponding author: Dr. Gopa Roy Biswas
Conflict of interest: Nil

Abstract

Lipid-based drug delivery systems are frequently employed as they may increase the solubility and bioavailability of lipophilic medications. An improved generation of lipid nanoparticles known as Nanostructured Lipid Carriers (NLCs) has the potential to overcome the disadvantages associated with conventional lipid-based formulations and solid lipid nanoparticles (SLNs). The current study employed Design-Expert® software (Version 7.1.5) to perform an optimization study using 2^3 Factorial design. The study involved Homogenizer Speed (RPM), the Amount of Liquid Lipid (mL), and the amount of Solid Lipid (g) as independent variables. The 8 formulations provided by the design software, were prepared by using hot homogenization technique. The Drug and other material's compatibility analysis were carried out using FTIR analysis. Dynamic light scattering (DLS) was used to measure the particle size of the NLC formulations. The Ex-vivo Drug Permeation Study was performed by using goat abdominal skin, obtained from slaughter's house, in the Franz Diffusion Cell. FTIR results stated that the excipients and the drug were compatible, as there were no significant changes of the peaks were noticed. The Particle Size of Formulations was in the range of 17.57 nm to 279.4 nm. The Entrapment efficiency of the NLC formulations was in the range of 63.1% to 98 %. The percentage of drug permeated from the formulations in 7 hours was in the range of 33.07 ± 0.00015 % to 61.86 ± 0.017%. According to this study, the optimized NLC fulfils the all criteria and is proven as a suitable topical drug delivery system.

Keywords: Nanostructured Lipid Carrier (NLC), 2^3 Factorial Design, Hot Homogenization Technique, Dynamic Light Scattering, Franz Diffusion Cell, Ex-vivo Permeation Study, Entrapment Efficiency.

Introduction

A topical drug delivery system is a way to provide medications topically, for therapeutic benefits on the skin. Pharmacists use the skin, one of the body's largest and most superficial organs, to deliver a variety of drugs. Since long ago, topical medicinal administration has been used to accomplish numerous goals at various levels. (Skin surface, epidermis, dermis, and hypodermis). However, there have been reports of several issues with standard topical treatments, including limited uptake because of the stratum corneum's barrier function and absorption into the bloodstream[1]. Nanotechnology is currently heavily utilizing drug delivery technology for passive and active targeting through a variety of administration techniques. Colloidal particulate systems between 10 and 1000 nm in size are considered nanoparticles[2]. To make NLCs, emulsifiers, suitable liquid and solid lipids, and biodegradable lipids are used. When liquid lipids (oil) are added to solid lipids, the crystalline structure becomes less ordered, which reduces drug leakage and allows for a large drug load[3]. The second generation of lipid nanoparticles, called nanostructured lipid carriers (NLCs), is formed of a combination of liquid oils and solid lipid matrices[4]. The size range of NLC is typically 200 to 400 nm. Various preparation methods lead to the various nanosize of NLC[5]. The upper nanosize range > 700 nm is shown to become less stable during long-term flocculation and creaming[6, 7]. Sizes smaller than 200 nm must be produced with higher surfactant concentrations, which are frequently undesired in formulations[8, 9]. However, because of recrystallization, NLCs that are 100 nm in size typically experience issues. On the other hand, NLCs with a size of 100 nm are of special interest for specific applications because of their better skin penetration[10,11]. Baiseng et al. (2013) created a technique for matching the essential hydrophilic-lipophilic balance (HLB) in the lipid phase in order to overcome this issue. NLC's solid matrix allows them to effectively immobilize medicines and stop particles from aggregating. As a result, the mobility of the drug molecules that have been integrated is significantly decreased in the solid phase[12–17]. Additionally, the solid matrix's liquid

oil droplets boost its ability to hold drugs while the lipid matrix's looser order allows for more effective drug accommodation[18].

Nowadays, lipid-based drug delivery techniques are frequently employed because they may increase the solubility and bioavailability of medications that are poorly water-soluble and/or lipophilic[19]. An improved generation of lipid nanoparticles known as NLCs has been developed, which has the potential to overcome the disadvantages associated with conventional lipid-based formulations and solid lipid nanoparticles. (SLNs)[20]. NLCs have become a practical carrier system for the delivery of pharmaceuticals via oral, parenteral, ophthalmic, pulmonary, topical, and transdermal routes[21]. Due to its distinct lipid composition and smaller particle size, NLC provides a tight contact with the stratum corneum, improving medication flow through the skin. Additionally, a regulated release of the medicinal moiety from these carriers is achievable because of the hardened lipid matrix[22]. NLCs can incorporate huge amounts of pharmaceuticals since they developed a less organized lipid matrix with many flaws. Due to a decrease in transepidermal water loss, they are also reported to exhibit occlusive qualities and considerably boost skin moisture[23]. SLNs incorporate the solid lipid, but NLCs entrap the drug in a mixture of solid and liquid lipids, thus resulting in a formulation with sustained release and eliminating the drawback of SLNs[24]. Terbinafine Hydrochloride is a mold-fighting synthetic allylamine antifungal. It is highly lipophilic and tends to accumulate in fatty tissues, the skin, and the nails[25]. Like other allylamines, terbinafine suppresses the production of ergosterol by impeding the activity of the enzyme squalene epoxidase, which is necessary for the manufacture of the fungal cell wall[26]. It is recommended to use terbinafine hydrochloride to treat fungal skin and nail infections caused by Trichophyton species, Microsporum canis, Epidermophyton floccosum, and Tinea species. Additionally, terbinafine hydrochloride treats skin yeast infections caused by Malassezia furfur and Candida species[27]. Terbinafine inhibits the enzyme squalene monooxygenase, preventing the conversion of squalene to 2, 3-oxydosqualene, which is the first step in the formation of ergosterol (also known as squalene epoxidase)[28]. Because of this inhibition, squalene accumulates and less ergosterol than would normally be synthesized is absorbed into the cell wall [29]. Squalene-containing cytoplasmic vesicles in large quantities may remove other lipids, causing additional harm to the cell wall[30, 31]. The goal of topical NLC formulation is to deliver the appropriate concentration to the target location to perform its therapeutic activity with the fewest possible side effects, although stability problems continue to be a source of worry[32]. When administered topically, many attempts have been made to increase the drug's bioavailability. NLCs, a more recent generation of SLNs, were thus chosen to get around these restrictions and offer stronger therapeutic prospects[33]. The goal of the current study was to prepare and optimize TH-loaded NLC for topical administration using the evaluation parameter of the formulations such as particle size, entrapment efficiency, and ex-vivo drug permeation study to determine whether it could be more efficient than the current topical delivery method for terbinafine hydrochloride.

Materials and Methods

Materials

Terbinafine Hydrochloride was obtained as a gift sample from Macleods Pharmaceuticals Ltd (Andheri East, Mumbai), and Stearic Acid from LOBA CHEMIE PVT.LTD (Mumbai, Maharashtra), Olive oil from BERTOLLI was purchased locally, and Tween 80 from Merck Specialties Private Limited (Shiv Sagar Estate 'A', Mumbai- 400 018) was chosen as the surfactant.

Compatibility Study of the Materials

The medicine (Terbinafine Hydrochloride) and other material (stearic acid, olive oil) compatibility analysis were carried out in this study using the FTIR study[34]. Terbinafine hydrochloride, stearic acid, olive oil, their physical mixtures, and Lyophilized product were investigated for their infrared transmission characteristics using an FT-IR spectrophotometer (Perkin Elmer Spectrum Two). The sample was created using the KBr pellet technique, and the FT-IR spectra were captured using an analyzer. Anhydrous KBr was combined with the samples at a mass ratio of 1:100 before being compacted into a thin pellet. After that, the samples were crushed into a powder. The pressure was 5.5 metric tons for three minutes under a hydraulic, while the scanning range was 3,500 - 500 cm-1[35].

Experimental Design

The current study employed Design-Expert® software (Version 7.1.5) to perform an optimization study using a three-factor two-level Factorial design[36]. The study involved two factors and Eight runs, with Homogenizer Speed (RPM), the Amount of Liquid Lipid (mL), and the amount of Solid Lipid (g) chosen as independent variables. The variables were set at high and low levels, and their coded values are presented in Table 1. Eight NLC formulations were prepared based on the plan, and their particle size (Y1), entrapment effectiveness (Y2), and % of Drug Permeated (Y3) were evaluated as response parameters[37].

Table 1: Different Independent Variables, Their Type, and Their Level Used in Experimental Design

Independent Variables	Unit	Type	Low	High
Amount of Liquid Lipid	mL	Numerical	2	4
Amount of Solid Lipid	g	Numerical	6	8
Homogenization Speed	RPM	Numerical	3000	8000

Methods of Preparation of TH_NF Formulations

Stearic acid, a solid lipid, and olive oil, a liquid lipid, were initially combined to create the lipid mixture using a magnetic stirrer (REMI 1MLH) from REMI ELEKTROTECHNIK LTD. in a heated environment (60°–70°C). (Vasai, India). Terbinafine Hydrochloride was also produced separately and heated to the same temperature in an aqueous form. The aqueous phase and lipid phase were then combined using a magnetic stirrer (REMI 1MLH) from REMI ELEKTROTECHNIK LTD. in a heated environment (60°–70°C) with a surfactant (tween 80). (Vasai, India). The mixture was run through a REMIMOTOR homogenizer (REMI ELEKTROTECHNIK LTD., Vasai, India) for 20 to 30 minutes at 300 to 8000 rpm. The temperature remained high during the procedure. Using an ultrasonic sonicator from LABMAN SCIENTIFIC INSTRUMENT PVT. LTD. (Chennai, 600118, India), the mixture was sonicated for 20 to 30 minutes before being left at room temperature for 48 hours.

The formulations were then lyophilized using an OPTICS TECHNOLOGY Lyophilizer (Delhi-34, India)[38–40]. The formulations and the amount of their all components are mentioned in Table 2.

Table 2: Composition of Different Formulations

Formulation	Olive oil (mL)	Stearic Acid (g)	Tween 80 (mL)	Terbinafine Hydrochloride (mg)	Distilled Water (mL)	Homogenization Speed
TH_NF1	4	8	0.6	30	15	3000
TH_NF2	2	8	0.6	30	15	3000
TH_NF3	2	6	0.6	30	15	3000
TH_NF4	4	8	0.6	30	15	8000
TH_NF5	4	6	0.6	30	15	3000
TH_NF6	2	6	0.6	30	15	8000
TH_NF7	2	8	0.6	30	15	8000
TH_NF8	4	6	0.6	30	15	8000

Characterization of TH_NF Formulation

Particle Size Determination

Using a Zetasizer Ver.7.11 (Malvern Instruments Ltd., UK), dynamic light scattering (DLS) was used to measure the particle size of the NLC formulations at 25 °C. The NLC formulations were dissolved in methanol of Merck Life Science Pvt. Ltd (Mumbai, India)[41]. They were examined for particle size and polydispersity index after being 100-fold diluted with methanol[42].

Entrapment efficiency (%)

By using a cooling-centrifugation technique, the EE% was found. 1 g of TH-NF was dissolved in 10 mL of pH-7.4 phosphate. With the use of a cooling centrifuge from REMI ELEKTROTECHNIK LTD. (Vasai, India), the dispersion was centrifuged at a low temperature (5-8ºC) for 20 minutes at 12,000 rpm[43]. The filter paper was used to filter the Supernatant liquid (Mess No. 11µm). The optical density was then determined using a UV spectrophotometer (JASCO, V630 Spectrophotometer) operating at a wavelength of 285 nm after the filtrate had been diluted. The medication concentration in the liquid supernatant was then determined using this information. Equation (1) was used to determine the EE%[44].

$$EE\% = \frac{Experimental\ Drug\ Content}{Theoritical\ Drug\ Content} \times 100 \text{--------- (1)}$$

Ex-vivo Permeation Study Using Goat Abdominal Skin

In the experiment, goat abdominal skin that had just been collected from the slaughterhouse was used. It was hydrated for an hour in a pH 7.4 PBS buffer [45].A Franz Diffusion Cell with a 45 ml capacity was employed for the Ex-vivo skin penetration study, as described. 1 g of the TH_NF formulations was applied to the stratum corneum of the goat's abdominal skin, which was facing the donor compartment. The skin was then positioned in the receiver compartment of the diffusion cell, which contained pH 7.4 PBS buffer. The temperature of the receptor solution was kept at 32 ± 0.5ºC throughout the experiment and a magnetic bead was used to agitate it continuously. The drug was evaluated after the samples were removed at various intervals of 15, 30, 60, 90, 120, 180, 240, 300, 360, and 420 minutes. A new buffer with a pH of 7.4 was introduced in place of the 4 ml of receptor solution that had been withdrawn. Using a UV-visible spectrophotometer

(JASCO, V630 Spectrophotometer) with a 285 nm wavelength, the samples' drug content was evaluated[46]. The computation was performed using the slope of the terbinafine hydrochloride standard curve in a pH-7.4 phosphate buffer. The following equation yields the slope (0.0074). y = 0.0074x and 0.9997 as the regression coefficient[47,48]. The UV-spectrophotometric data were used to calculate the ratio of the retained drug to the penetrated drug[49, 50].

Optimization of TH_NF formulations

Using Design-Expert® software (Version 7.1.5), the TH_NF formulations were improved in terms of the response, such as particle size, entrapment effectiveness, and % of drug permeates. The 2FI model was initially chosen for study. The model was then examined using the ANOVA and R-squared tests. The layout demonstrated how the independent parameters affected particle size, entrapment effectiveness, and % of drug permeates independently (A or B, or C), and in combination (AB or AC, or BC). Plots of the three-dimensional response surface, for example, the conclusion of the design represented via polynomial equations and 3D response graphs. Numerical optimization led to the discovery of optimized solutions as optimized products, and among them, one formulation was chosen for further evaluation of the optimized product based on smaller particle size and higher entrapment efficiency, and higher permeation.

Results and Discussion

Compatibility Study of the Materials

Terbinafine Hydrochloride and Excipients (Stearic Acid and Olive Oil) were tested for any physical or chemical interactions using FTIR studies, and the FTIR spectrum is displayed in Figure 1. In the Terbinafine Hydrochloride FTIR spectrum, the C-C in the ring and Ar_2NH groups were all discernible; their stretch bands for Ar-N and C-C were located at 1490 $cm^{-1}$and 1326 cm^{-1}, respectively. C-C in the ring, Ar_2NH, RCOOH, and RCOOR1 had stretched bands that were at 1448 cm^{-1}, 1324 cm^{-1}, 1131 cm^{-1}, and 1045 cm-1, respectively, just like the physical mixture of Terbinafine Hydrochloride, Stearic Acid, and Olive Oil. The Lyophilized product shows stretched bands at 1448 cm^{-1}, 1324 cm^{-1}, 1131 cm^{-1}, and 1045 cm^{-1} for C-C in the ring, Ar_2NH, RCOOH, and RCOOR1 functional groups. These common transmission bands clearly showed that there was no physical or chemical interaction between the drug, olive oil, or stearic acid. The excipients and the drug were a perfect match

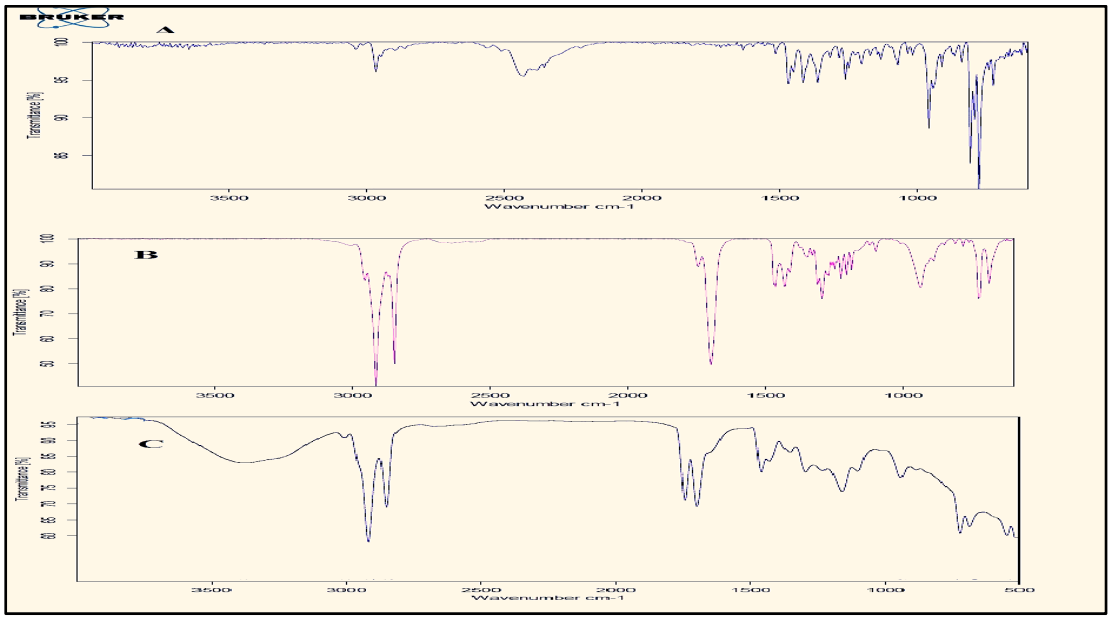

Figure 1: FTIR spectra of (A) Drug (B) Drug + All Excipients (C) Lyophilized Product

Characterization of TH_NF Formulation

Particle size determination

The results of the investigation into the particle size of the synthesized TH_NF formulations are displayed in Table 3 and Figure2 and the Particle size distribution was also shown in Figure 2. The NLC was prepared by using the hot homogenization technique. Dynamic light scattering was employed to figure out the size of the particles of the NLC Formulations. The Particle Size of Formulations was in the range of 17.57 nm (TH_NF8) to 279.4 (TH_NF3).

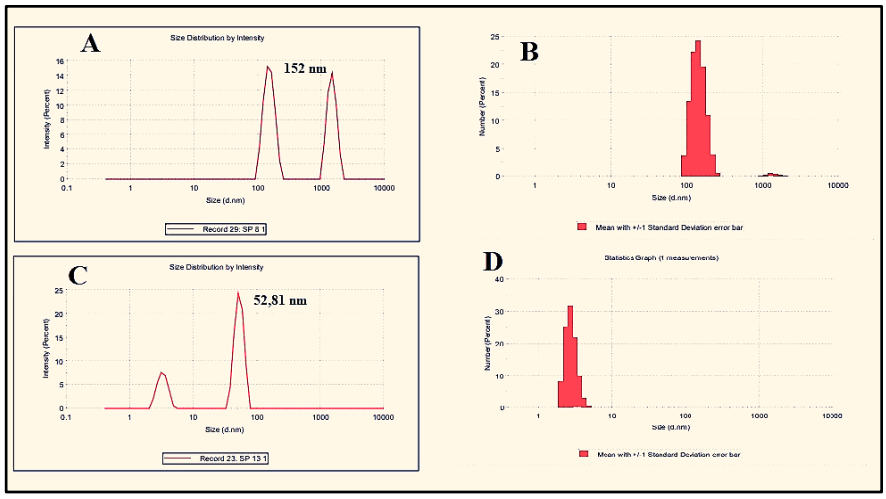

Figure 2: DLS Result of TH_NF formulation (A) Particle Size of TH_NF1 (B) Size Distribution of TH_NF1 (C) Particle Size of TH_NF4 (D) Size Distribution of TH_NF4

Entrapment Efficiency (%)

The prepared TH_NF formulation's entrapment efficiency was calculated using the indirect method, and the results are displayed in Table 3. The Entrapment efficiency of the TH_NF formulations was in the range of 63.1% (TH_NF2) to 98 % (TH_NF4).

Ex-vivo Permeation Study Using Goat Abdominal Skin

The Ex-vivo permeation profile of Terbinafine Hydrochloride from the TH_NF formulations is shown in Figure 3. The results are shown in Table 3. The outcomes demonstrate that the drug diffusion from the TH_NF formulations exhibits biphasic behavior, it steadily increased and maintained a steady pace after 6 hours. The Ex-vivo Drug Permeation Study of the formulations was performed by using goat abdominal skin. The % of drug permeated from the formulations in 7 hours was in the range of 33.07 ± 0.00015% to 61.86 ± 0.017%. The permeation coefficient of the different formulations was calculated with the help of the equation: P = K*Vr/S, where, S is the effective Surface area of goat abdominal skin, Vr is the volume of the receiver chamber, K is the Zero-order constant, P is permeability coefficient[45]. The R^2 values, Permeability Coefficients, and Flux for different formulations are mentioned in Table 4.

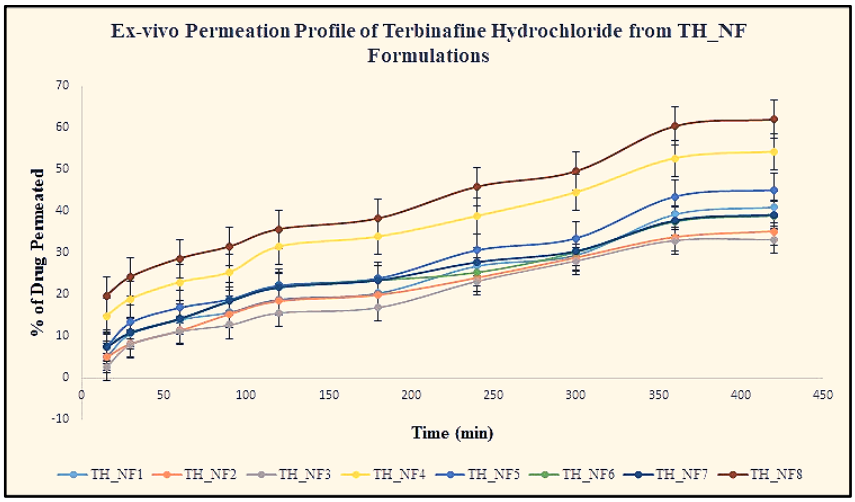

Figure 3: Ex-vivo Permeation Profile of Terbinafine Hydrochloride from 8 TH_NF Formulations

Table 3: Particle Size, Entrapment Efficiency, and % of Drug Permeation of Different TH_NF Formulation

Formulation	Particle Size (nm)	Entrapment Efficiency (%)	% of Drug Permeated (± SD, N=3) in 7 hours
TH_NF1	152	85	40.98 ± 0.010
TH_NF2	259.9	63.1	35.11 ± 0.040
TH_NF3	279.4	75	33.07 ± 0.00015
TH_NF4	52.81	98	54.19 ± 0.031

TH_NF5	134	93.33	44.97 ± 0.016
TH_NF6	174	92	38.84 ± 0.041
TH_NF7	154	91.33	39.05 ± 0.019
TH_NF8	17.57	95.33	61.86 ± 0.017

Table 4: R^2 values, Permeability Coefficients, and Fluxs of Different Formulations

Formulations	R^2 Value	Permeability Coefficient (cm/min)	Flux (mg/cm^2/min)
TH_NF1	0.9715	419.62	0.0818
TH_NF2	0.9722	403.57	0.0716
TH_NF3	0.9664	306.12	0.0721
TH_NF4	0.9807	944.14	0.0949
TH_NF5	0.9722	570.95	0.0858
TH_NF6	0.9619	555.48	0.0724
TH_NF7	0.9670	558.34	0.0738
TH_NF8	0.9820	1216.38	0.1007

Optimization of TH_NF formulations

To determine the optimal NLC formulation with the lowest particle size, the highest entrapment effectiveness, and the highest drug permeation, a three-factor, two-level Factorial formulation design approach was applied. 8 formulation compositions were obtained from the design to look for flaws in the outcomes. To interpret the results, the particle size (Y1), entrapment effectiveness (Y2), and % of drug permeated (Y3) data were taken into account. To evaluate the effects of independent factors on dependent components, the software generated predicted values, polynomial equations, and 3D response surface graphs. The outcome was found to be closer to the projected value when the anticipated value generated by the program was compared to the actual particle size, entrapment efficiency, and % of Drug Permeation. The 2FI model with the highest correlation coefficient for all responses was found to be the best-fit model (R2) (Table 5). The 2FI response was best for optimization because the selected independent variable affected the dependent variables both individually and collectively. The ANOVA result was deemed to be significant because the F value showed a value greater than 4. Residual values were discovered to support the optimization (Table 6). While the polynomial equation's negative value indicates the opposite relationship, its positive sign promotes the interaction of independent factors with the dependent variables. Since the total combined desirability was found to be closer to unity, it was decided that the tested independent variable was appropriate for the optimization.

Table 5: Statistical model summary of regression analysis results for responses Y1, Y2, and Y3

Model	R^2	Adjusted R^2	Predicted R^2	SD	%CV	Remark
Particle Size (Y1)						
Linear	0.9796	0.9644	0.9186	16.97	11.09	
2FI	0.9993	0.9951	0.9555	6.27	4.01	Suggested
Quadratic	-	-	-	-	-	Aliased
Cubic	-	-	-	-	-	Aliased
Entrapment Efficiency (Y2)						
Linear	0.8166	0.6791	0.2665	6.74	7.79	
2FI	1.0000	1.0000	0.9996	0.081	0.094	Suggested
Quadratic	-	-	-	-	-	Aliased
Cubic	-	-	-	-	-	Aliased
% of Drug Permeated (Y3)						
Linear	0.8819	0.7933	0.5276	4.48	10.30	
2FI	0.9994	0.9956	0.9598	0.65	1.50	Suggested
Quadratic	-	-	-	-	-	Aliased
Cubic	-	-	-	-	-	Aliased

Table 6: ANOVA of quadratic model for responses of developed TH_NFs

ANOVA Results	Particle Size (nm) (Y1)	Entrapment Efficiency (%) (Y2)	% of Drug Permeated (Y3)
Regression			
Some of square	56548.54	992.35	680.14
Degree of freedom	6	6	6
Mean square	9424.76	165.39	113.36
F-value	239.58	25012.04	264.97
P	0.0494	0.0048	0.0470
Influence	Significant	Significant	Significant
Residual			
Some of square	39.34	6,613E-003	0.43
Degree of freedom	1	1	1
Mean square	39.34	6,613E-003	0.43

Effect of Independent Variables on Particle Size (Y1), Entrapment Efficiency (Y2), and % of Drug Permeated (Y3)

The results of the particle size (Y1), entrapment efficiency (Y2), and % of Drug Permeated (Y3) analyses were analyzed using the ANOVA and R-squared tests, and the relationship between the independent variables, particle size, and entrapment efficiency was described by the following equations (2), (3), and (4) obtained after analyzing the results of particle size and entrapment efficiency analyses, respectively, as well as by the 3D-Response curve.

Particle Size (Y1) = + 152.96 - 63.87 * A + 1.72 * B -53.37 * C + 11.59 * A * B - 0.54 * A * C + 2.0 * B * C ----- (2)

Entrapment Efficiency (Y2) = + 86.64 + 6.28 * A - 2.28 * B + 7.53 * C + 0.86 * A * B - 3.78 * A * C + 2.78 * B * C -------- (3)

% of Drug Permeated (Y3) = + 43.51+ 6.99 * A – 1.18 * B + 4.98 * C - 1.74 * A * B + 2.55 * A * C - 0.69 * B * C -------- (4)

According to equation [2], the amount of liquid lipid (A) had a negative impact on particle size. According to the equation, when the amount of liquid lipid was reduced, the particle size increased; this is likely because the homogenization speed varied. Additionally, it was discovered that the amount of solid lipid (B) had a positive impact on particle size. According to the equation, particle size grows as the amount of solid lipid speed grows. The equation also described that homogenization speed (C) had a negative effect on particle size which means when the homogenization speed was reduced the particle size was increased. The particles of the formulations may agglomerate at high homogenization speeds. The amount of liquid lipid and the amount of solid lipid (AB) together had a beneficial impact on particle size. Therefore, the equation demonstrates that both the amount of solid lipid and the amount of liquid lipid had a significant impact on particle size. The amount of liquid lipid and homogenization speed (AC) together had a negative impact on particle size. Therefore, the equation demonstrates that the amount of liquid lipid had a significant impact on particle size. The amount of solid lipid and homogenization speed (BC) together had a positive impact on particle size. Therefore, the equation demonstrates that both the amount of solid lipid and homogenization speed had a significant impact on particle size. The effect of the independent variables on the particle size was shown in the 3D response graph (Figure 4).

According to equation [3], the amount of liquid lipid (A) had a positive impact on the entrapment efficiency. According to the equation, the entrapment efficiency increased when the amount of liquid lipid was increased. It was also discovered that the amount of solid lipid (B) had a negative impact on the entrapment efficiency. According to the equation, the amount of solid lipid rose along with the entrapment efficiency. The equation also described that homogenization speed (C) had a positive effect on entrapment efficiency which means when the homogenization speed was increased the entrapment efficiency was increased. The amount of liquid lipid and the amount of solid lipid (AB) together had a positive impact on entrapment efficiency. As a result, the equation demonstrates that the amount of solid lipid and liquid lipid had a significant impact on entrapment efficiency. The amount of liquid lipid and homogenization speed (AC) together had a negative impact on entrapment efficiency. Therefore, the equation demonstrates that the amount of liquid lipid had a significant impact on entrapment efficiency. The amount of solid lipid and homogenization speed (BC) together had a positive impact on entrapment efficiency. Therefore, the equation demonstrates that both the amount of solid lipid and homogenization speed had a significant impact on entrapment efficiency. The effect of the independent variables on the entrapment efficiency was shown in the 3D response graph (Figure 4).

According to equation [4], the amount of liquid lipid (A) had a positive impact on the % of drug permeated. According to the equation, the % of drug permeated increased when the amount of liquid lipid was increased. It was also discovered that the amount of solid lipid (B) had a negative impact on the % of drug permeated. According to the equation, the amount of solid lipid rose along with the % of drug permeated. The equation also described that homogenization speed (C) had a positive effect on % of drug permeated which means when the homogenization speed was increased the % of drug permeated was increased. The amount of liquid lipid and the amount of solid lipid (AB) together had a negative impact on % of drug permeated. As a result, the equation demonstrates that the amount of solid lipid had a significant impact on % of drug permeated.

The amount of liquid lipid and homogenization speed (AC) together had a positive impact on % of drug permeated. Therefore, the equation demonstrates that both the amount of liquid lipid and homogenization speed had a significant impact on % of drug permeated. The amount of solid lipid and homogenization speed (BC) together had a negative impact on % of drug permeated. Therefore, the equation demonstrates that the amount of solid lipid had a significant impact on % of drug permeated. The effect of the independent variables on % of drug permeated was shown in the 3D response graph (Figure 4).

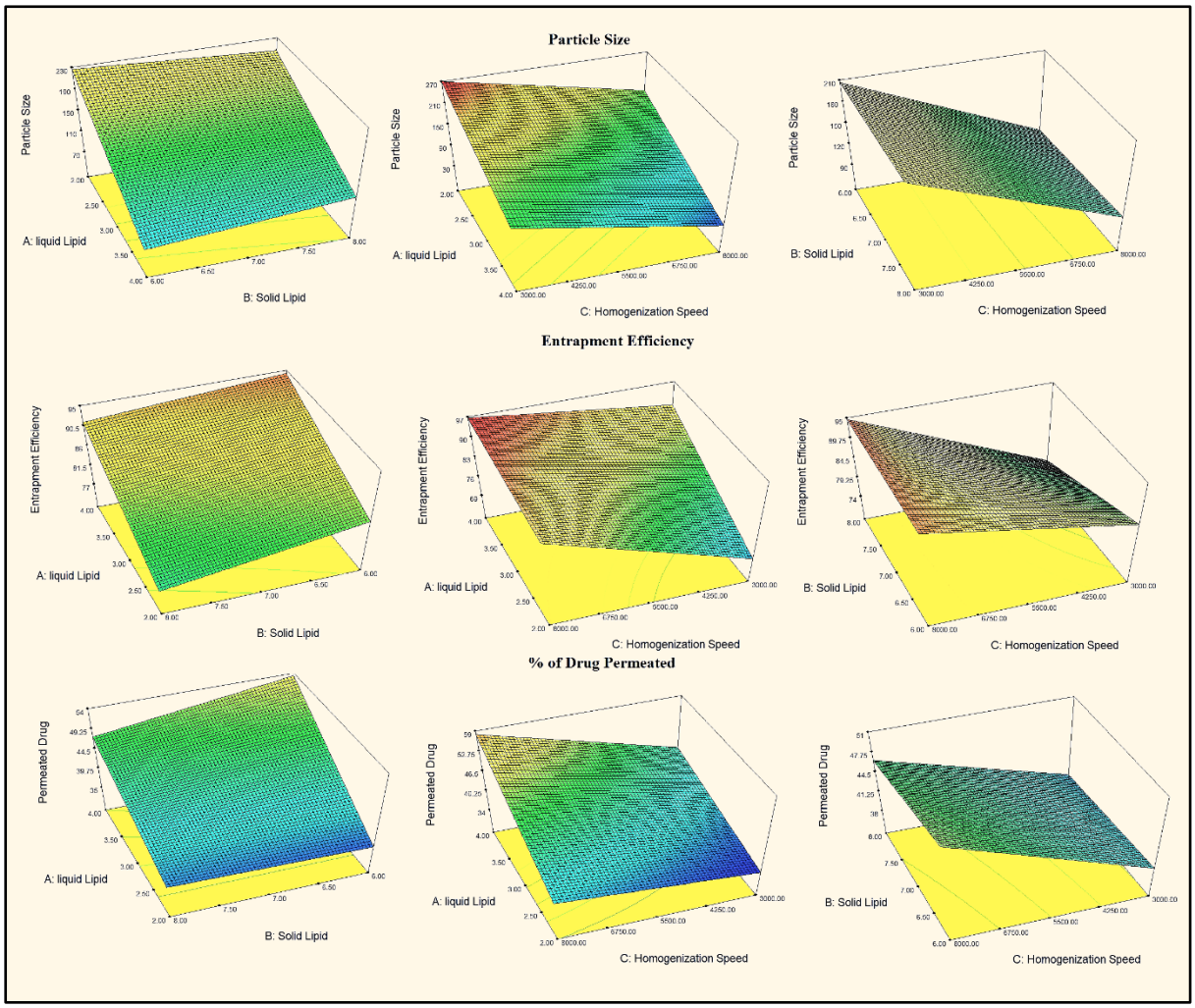

Figure 4: 3D Response Curve Showing Effect of Independent Variables on Particle Size, Entrapment Efficiency, and % of Drug Permeated.

The 38 solutions were discovered as the optimized products after doing the numerical optimization. The solution with the lowest particle size, highest entrapment efficiency, and highest drug permeation out of these 38 formulations was chosen as the optimized product ($TH\_NF_{opt.}$), which is identical to TH_NF8. The optimized formulation has a particle size of 17.57 nm, entrapment efficiency of 95.33%, and the % of drug permeated from the optimized formulation was 61.86 ± 0.017%. The study lacked stability, antifungal, and irritation studies, which can be performed in the future to further evaluate optimized formulation for use in topical drug delivery. Consequently, based on the results of the study performed here, we can state that the NLC

formulations have an effective action on the delivery of antifungal drugs through the skin.

Conclusion

In this study, a three-factor, two-level Factorial design was used to develop and optimize the Terbinafine Hydrochloride loaded nanostructured lipid carrier formulation (TH_NF) concerning three response parameters, particle size, entrapment efficiency, and % of drug permeated. Obtained 8 formulations from the experimental design were prepared by adopting most relevant technique i.e., hot homogenization method. The prepared formulation were subjected to different evaluation tests for continuation of the optimization study. The optimized formulation was selected based on lower particle size, higher entrapment efficiency, and higher % of drug permeated. The DOE software provided thirty-eight optimised formulations. Among them the lowest particle size with all the satisfactory results were considered for Ex-vivo permeation study to confirm the proper application of topical formulations.

Acknowledgements: The facilities required to conduct the research were provided by Guru Nanak Institute of Pharmaceutical Science and Technology, Kolkata, for which the authors are grateful. They are particularly appreciative of the experimental support for DLS provided by the Bose Institute, Kolkata.

References

1. Abdo JM, Sopko NA, Milner SM. The applied anatomy of human skin: A model for regeneration. Wound Medicine 2020; 28:100179.
2. Alam MS, Algahtani MS, Ahmad J, et al. Formulation design and evaluation of aceclofenac nanogel for topical application. Therapeutic Delivery. 2020;11(12):767-778.
3. Azhar SNAS, Ashari SE, Zainuddin N, et al. Nanostructured Lipid Carriers-Hydrogels System for Drug Delivery: Nanohybrid Technology Perspective. Molecules. 2022;27 (1):289.
4. Zauner W, Farrow NA, Haines AMR.. In vitro uptake of polystyrene microspheres: Effect of particle size, cell line and cell density. Journal of Controlled Release. 2001; 71(1):39–51.
5. Shidhaye S, Vaidya R, Sutar S et al. Solid Lipid Nanoparticles and Nanostructured Lipid Carriers – Innovative Generations of Solid Lipid Carriers. Current Drug Delivery. 2008; 5(4): 324–331.
6. Müller RH, Radtke M, Wissing SA. Solid lipid nanoparticles (SLN) and nanostructured lipid carriers (NLC) in cosmetic and dermatological preparations. Advanced Drug Delivery Reviews. 2002; 54:131–155.
7. Alam T, Pandit J, Vohora D, et al. Optimization of nanostructured lipid carriers of lamotrigine for brain delivery: In vitro characterization and in vivo efficacy in epilepsy. Expert Opinion on Drug Delivery. 2015; 12(2):181–194.
8. Pardeike J, Weber S, Haber T, et al. Development of an Itraconazole-loaded nanostructured lipid carrier (NLC) formulation for pulmonary application. International Journal of Pharmaceutics. 2011;419(1–2):329–38.
9. Shit SC, Shah PM. Edible Polymers: Challenges and Opportunities. Journal of Polymers. 2014;2014: 1–13.
10. Kadajji VG, Betageri G V. Water soluble polymers for pharmaceutical applications. Polymers. 2011; 3(4):1972–2009.
11. Zohdi RM, Zakaria ZAB, Yusof N, et al. Sea cucumber (Stichopus hermanii) based hydrogel to treat burn wounds in rats. Journal of Biomedical Materials Research - Part B Applied Biomaterials2011; 98 B(1): 30–37.
12. Yang JM, Su WY, Leu TL et al. Evaluation of chitosan/PVA blended hydrogel membranes. Journal of Membrane Science2004; 236 (1-2): 39–51.
13. Knop K, Hoogenboom R, Fischer D, et al. Poly(ethylene glycol) in drug delivery: Pros and cons as well as potential alternatives. Angewandte Chemie - International Edition.2010.; 49(36): 6288–6308.
14. Liu CH, Wu CT. Optimization of nanostructured lipid carriers for lutein delivery. Colloids and Surfaces A: Physicochemical and Engineering Aspects2010;353(2-3):49–156.
15. Das S, Chaudhury A. Recent advances in lipid nanoparticle formulations with solid matrix for oral drug delivery. AAPS PharmSciTech2011; 12(1); 62–76.
16. Pardeike J, Hommoss A, Müller RH. Lipid nanoparticles (SLN, NLC) in cosmetic and pharmaceutical dermal products. International Journal of Pharmaceutics. 2009; 366(1-2): 170–184.
17. Araújo J, Gonzalez E, Egea MA, et al. Nanomedicines for ocular NSAIDs: safety on drug delivery. Nanomedicine: Nanotechnology, Biology, and Medicine. 2009; 5(4):394–401.
18. Jaiswal P, Gidwani B, Vyas A. Nanostructured lipid carriers and their current application in targeted drug delivery. Artificial Cells, Nanomedicine and Biotechnology2016; 44(1):27–40.
19. Chauhan I, Yasir M, Verma M, et al. Nanostructured lipid carriers: A ground breaking approach for transdermal drug delivery. Advanced Pharmaceutical Bulletin. 2020; 10:150–165.
20. Dubey A, Prabhu P, Kamath J V. Nano structured lipid carriers: A novel topical drug delivery system. International Journal of Pharm Tech Research. 2012; 4(2):705-714.
21. Chutoprapat R, Kopongpanich P, Chan LW. A

Mini-Review on Solid Lipid Nanoparticles and Nanostructured Lipid Carriers: Topical Delivery of Phytochemicals for the Treatment of Acne Vulgaris. Molecules. 2022; 27:3460.
22. Waghule T, Rapalli VK, Gorantla S, et al. Nanostructured Lipid Carriers as Potential Drug Delivery Systems for Skin Disorders. Current Pharmaceutical Design. 2020; 26(36):4569-4579.
23. Patil TS, Gujarathi NA, Aher AA, et al.. Recent Advancements in Topical Anti-Psoriatic Nanostructured Lipid Carrier-Based Drug Delivery. International Journal of Molecular Sciences. 2023; 24:2978.
24. Saez V, Souza IDL, Mansur CRE. Lipid nanoparticles (SLN & NLC) for delivery of vitamin E: a comprehensive review. International Journal of Cosmetic Science. 2018; 40: 103-116.
25. Paliwal S, Kaur G. Formulation And Characterization of Topical Nano Emulgel of Terbinafine. Universal Journal of Pharmaceutical Research. 2019; 3(6).
26. Thavva V, Baratam SR. Formulation and evaluation of terbinafine hydrochloride microsponge gel. International Journal of Applied Pharmaceutics. 2019;11(6):78-85.
27. Iizhar SA, Syed IA, Satar R, et al. In vitro assessment of pharmaceutical potential of ethosomes entrapped with terbinafine hydrochloride. Journal of Advanced Research. 2016;7(3):-453-461.
28. Szabó P, Daróczi TB, Tóth G, et al. In vitro and in silico investigation of electrospun terbinafine hydrochloride-loaded buccal nanofibrous sheets. Journal of Pharmaceutical and Biomedical Analysis. 2016;131:156-159.
29. Yang Y, Ou R, Guan S, et al. A novel drug delivery gel of terbinafine hydrochloride with high penetration for external use. Drug Delivery. 2015;22(8):1086-1093.
30. Gul U, Khan MI, Madni A, et al. Olive oil and clove oil-based nanoemulsion for topical delivery of terbinafine hydrochloride: in vitro and ex vivo evaluation. Drug Delivery. 2022; 29(1): 600-6012.
31. Gaba B, Fazil M, Khan S, et al. Nanostructured lipid carrier system for topical delivery of terbinafine hydrochloride. Bulletin of Faculty of Pharmacy, Cairo University. 2015; 53(2):147-159.
32. Doktorovova S, Souto EB. Nanostructured lipid carrier-based hydrogel formulations for drug delivery: A comprehensive review. Expert Opinion on Drug Delivery. 2009 ;6(2):165-76.
33. Tapeinos C, Battaglini M, Ciofani G. Advances in the design of solid lipid nanoparticles and nanostructured lipid carriers for targeting brain diseases. Journal of Controlled Release. 2017; 264:306-332.
34. Anwar W, Dawaba HM, Afouna MI, et al. Enhancing the oral bioavailability of candesartan cilexetil loaded nanostructured lipid carriers: In vitro characterization and absorption in rats after oral administration. Pharmaceutics. 2020; 12(11):1047.
35. Teng Z, Yu M, Ding Y, et al. Preparation and characterization of nimodipine-loaded nanostructured lipid systems for enhanced solubility and bioavailability. International Journal of Nanomedicine. 2019. ;14:119–133.
36. Singh P, Singh M, Kanoujia J, et al. Process optimization and photostability of silymarin nanostructured lipid carriers: effect on UV-irradiated rat skin and SK-MEL 2 cell line. Drug Delivery and Translational Research. 2016 ;6(5):597-609.
37. Khurana S, Jain NK, Bedi PMS. Development and characterization of a novel controlled release drug delivery system based on nanostructured lipid carriers gel for meloxicam. Life Sciences. 2013;93(21):763-72.
38. Mahmood A, Rapalli VK, Gorantla S, et al. Dermatokinetic assessment of luliconazole-loaded nanostructured lipid carriers (NLCs) for topical delivery: QbD-driven design, optimization, and in vitro and ex vivo evaluations. Drug Delivery and Translational Research. 2022;12(5): 1118-1135.
39. Sethuraman N, Shanmuganathan S, Sandhya K, et al. Design, development and characterization of nano structured lipid carrier for topical delivery of aceclofenac. Indian Journal of Pharmaceutical Education and Research. 2018; 52(4):581–586.
40. Riaz A, Hendricks S, Elbrink K, et al Preparation and Characterization of Nanostructured Lipid Carriers for Improved Topical Drug Delivery: Evaluation in Cutaneous Leishmaniasis and Vaginal Candidiasis Animal Models. AAPS Pharm Sci Tech. 2020;21(5):185.
41. Badawi NM, Elkafrawy MA, Yehia RM, et al. Clinical comparative study of optimized metronidazole loaded lipid nanocarrier vaginal emulgel for management of bacterial vaginosis and its recurrence. Drug Delivery2021; 28(1): 814-825.
42. Tran TH, Ramasamy T, Truong DH, et al. Preparation and Characterization of Fenofibrate-Loaded Nanostructured Lipid Carriers for Oral Bioavailability Enhancement. AAPS Pharm Sci Tech. 2014; 15(6):1509–1515.
43. Mahdi WA, Bukhari SI, Imam SS, et al. Formulation and optimization of butenafine-loaded topical nano lipid carrier-based gel: Characterization, irritation study, and anti-fungal activity. Pharmaceutics. 2021; 13(7):1087.

44. Permanadewi I, Kumoro AC, Wardhani DH, et al. Modelling of controlled drug release in gastrointestinal tract simulation. In Journal of Physics: Conference Series. 12952019: 1-8.
45. Biswas GR, Majee SB, Roy A. Combination of synthetic and natural polymers in hydrogel: An impact on drug permeation. Journal of Applied Pharmaceutical Science. 2016; 6(11):158–164.
46. Rao S, Barot T, Rajesh KS, et al. Formulation, optimization and evaluation of microemulsion based gel of Butenafine Hydrochloride for topical delivery by using simplex lattice mixture design. Journal of Pharmaceutical Investigation. 2016. 46(1):1-12.
47. Puri V, Froelich A, Shah P, et al. Quality by Design Guided Development of Polymeric Nanospheres of Terbinafine Hydrochloride for Topical Treatment of Onychomycosis Using a Nano-Gel Formulation. Pharmaceutics. 2022; 14(10):2170.
48. Hassan S ul, Khalid I, Hussain L, et al. Development and Evaluation of pH-Responsive Pluronic F 127 Co-Poly- (Acrylic Acid) Biodegradable Nanogels for Topical Delivery of Terbinafine HCL. Dose-Response. 2022; 20(2).
49. Biswas GR, Chakraborty S, Ghosh N, et al. Fabrication of bucco-matrix tablets of Amoxicillin trihydrate on the basis of release and permeation kinetics. Journal of Applied Pharmaceutical Science. 2015; 5(4); 48–52.
50. Sandeep DS, Mahitha M, Meghna S. Development, Characterization, and In vitro Evaluation of Aceclofenac Emulgel. Asian Journal of Pharmaceutics. 2020; 14(3).